International Journal of Robotics and Control Systems
Vol. 5, No. 2, 2025, pp. 730-747
ISSN 2775-2658
http://pubs2.ascee.org/index.php/ijrcs

Hybrid Deep Learning Model for Hippocampal Localization in Alzheimer's Diagnosis Using U-Net and VGG16

Fallah H. Najjar [a,b,1,*], Nawar Banwan Hassan [c,2], Salman Abd Kadum [a,3]

[a] Department of Computer Systems Techniques, Technical Institute of Najaf, Al-Furat Al-Awsat Technical University, 54001, Iraq
[b] Department of Emerging Computing, Faculty of Computing, Universiti Teknologi Malaysia, Johor Bahru 81310, Malaysia
[c] Department of Computer Engineering Techniques, Imam Alkadhim University College, Baghdad, Iraq
[1] fallahnajjar@atu.edu.iq; [2] nawarbanwan@alkadhum-col.edu.iq; [3] salman.kadhum@atu.edu.iq
* Corresponding Author

ARTICLE INFO

Article history
Received December 07, 2024
Revised January 10, 2025
Accepted February 06, 2025

Keywords
Alzheimer;
VGG16;
U-Net Autoencoder;
Localization;
Hippocampus

ABSTRACT

Alzheimer's disease (AD) is a complex neurodegenerative disease that involves considerable challenges in accurately diagnosing and locating the affected brain regions. This paper proposes a new fusion model based on VGG16 and U-Net to achieve accurate segmentation of hippocampus localization and improve AD diagnostic accuracy. Compared to previous techniques such as hierarchical fully convolutional networks (FCNs) or LBP-TOP localization (an accuracy range of 68% to 95%), our approach achieved a superior accuracy (98.6%) with a mean Jaccard index of 97.3%, like the predicted accuracy range of conventional imaging analysis techniques. By utilizing pre-trained transfer learning models and sophisticated data augmentation methods, generalization to different datasets greatly reduced over-fitting. Although existing approaches usually require labor-intensive segmentation or employ handcrafted features, our model automates the hippocampus's localization, leading to improved efficiency and scalability. The effectiveness of our method is strongly supported by the performance metrics including Mean Squared Error (MSE) and Avg. error Standard Deviation which show that MSE values were 5 times lower than those produced using the Hough-CNN based approach (0.0507 vs. 4.4%). Real-world demands include the need for minimal computational complexity and dependence on pre-processed ADNI MRI datasets compromising generalizability in actual clinical frameworks. Our results demonstrated that the fusion model yields superior hippocampal segmentation performance and a new standard for AD diagnostic scores, making a substantial impact on both academic and clinical domains.

1. Introduction

Alzheimer's Disease (AD) is a chronic, progressive and irreversible degeneration of the brain that leads to the gradual decline of thought and memory function and eventually affects behavior [1]. The most common cause of dementia. The progressive impairment of cognitive abilities such as logic, problem solving, and memory characterizes the disorder. These handicaps disrupt an individual's ability to perform everyday activities and much of their quality of life [2]. Most often seen in those

over 65, Alzheimer's becomes more common with increasing age. While aging is the single biggest risk factor, Alzheimer's is problematic and life-threatening to those who have it but not normal for old age. It is a distinct clinical illness caused by complex changes in the brain, including abnormal protein buildup and the loss of cells. In addition to the devastation of the person living with the disease, Alzheimer's can affect the lives of whole families and caregivers since this chronic illness usually requires long-term care combined with emotional support [3]. AD is a pressing global health matter, with its prevalence increasing steadily because of the worldwide aging population. AD is a burden that grows heavier all the time, which has caused urgent problems for not only individual patients but also health care systems, which have to tackle the widespread phenomenon of its development [4]. The progression of AD involves a steady breakdown of the brain, moving through several obvious stages in a process frequently described as ``conversion" or progression. To correctly diagnose and treat Alzheimer's disease, it is essential to know these stages well [5], [6]. The first stage, Clinical Normal (CN), is marked by a complete lack of identifiable cognitive symptoms. During this phase, people have normal memory and thinking skills. As for underlying changes in the brain wrought by AD or, for that matter, any other disorder, there is no evidence yet of loss of day-to-day function to carry this through into consciousness. That is why, at this stage, one does not stand a chance to receive a clear-cut clinical diagnosis based solely on symptoms. The second phase of brain conditions is Mild Cognitive Impairment (MCI), also known as the pre-dementia stage. In this stage, individuals undergo subtle but measurable declines in cognitive capabilities, such as memory or problem-solving, which may be noticed by themselves or others. However, these declines are not so bad as to seriously impair everyday life [7]. MCI is of particular significance since it is a higher-risk phase for the development of Alzheimer's disease (AD). Some research has found that about 7% of people with MCI go on to AD every year [8], [9]. MCI can be further divided into two kinds [10]. The first is progressive MCI (pMCI), where the continued decline in cognitive function eventually leads to AD, and stable MCI (sMCI), which remains at that level without further progress [11], [12]. Identifying these different types is very important, as it allows healthcare personnel to determine who is most at risk for advancement and explore possible interventions that could slow or delay the onset of AD. Early identification and better management of AD depends on being able to identify as early as possible the transition from CN to MCI and beyond stage dementia.

A key area of focus for researchers is finding effective ways to distinguish between sMCI and pMCI. With this in mind, doctors will be better able to look for indicators that these MCI patients will almost certainly progress to AD. Early detection of high-risk patients is paramount because it allows doctors to intervene and treat more effectively [8], [13]. Many studies have looked in depth at how AD develops. The primary purpose of these studies is to track its progress over time and identify the specific changes and abnormalities occurring in the brain. To predict how the disease will advance, more material is required: a comprehensive understanding of what exactly these abnormalities are and the driving factors for AD progression [14]. This could also indicate that the AD pathology accumulates during cognitive vitality [15]. This means that the AD pathology develops while the individual is still cognitive. However, recently, pMCI versus sMCI differentiation is based on neuroimaging biomarkers and cognitive tests with varied accuracy and inconsistent reliability, which highlights the need for more effective approaches [16]. The limited tools available for the prognostication of MCI to AD conversion emphasize the importance of new modalities capable of quantifying residual subclinical changes in brain structure and their relationship to clinical diagnosis [9], [17], [18].

It is difficult to generate a sound model for formally specifying software development since there is no consensus on how this can be done. It may be more accurate to say that the entire process can benefit from some form of induction. The downside of this idea is that engineers are not very well equipped to attempt to help build software programs [19], [20]. Manual localization is highly dependent on operator skills, with most needing the experience of a radiologist, resulting in labor-intensive and expensive solutions [21]. In contrast, spatial relation-based approaches use specific rules predefined in terms of, e.g., a fuzzy system to estimate location [22]. These are the atlas-based approaches, which automate localization but require an available reference base to be taken from and

thus utilized in the target data set through co-registration protocols [23]. While providing exact automatic localization, this approach usually requires considerable computational time and data [19]. Therefore, more recently, researchers have been considering alternative approaches including statistical shape model-based techniques [24], [25], which are capable of predicting the variations in shapes within a training population. This captures the mean approximate shape among all shapes seen in training data, and then parameterizes it. Statistical Shape Model based approaches make use of this mean shape to estimate the average location of the target anatomy [26]. Basher et al. [19] proposed an integration of a Hough voting scheme along with a convolutional neural network for addressing this issue on automatic localization of brain anatomical structures, particularly the Hippocampus. The authors report the utilization of a deep convolutional neural network (CNN) to calculate displacement vectors for the Hough voting strategy over many 3-viewpoint patch samples. They combined these displacement vectors with the positions of our sample to estimate where the target would be. To learn effectively from such samples, a dual local and global strategy was employed. To do this, we trained multiple local models with patches of the neighborhood around each hippocampus point and combined them into a perfused prediction. Furthermore, Basher et al. [23] proposed a discrete volume size from volumetric MRI scans of the Hippocampus and removed dependence on prior segmentation by used deep learning-based method of objectively quantifying. They used an approach to develop a 2 dimensional CNN model with three channel of 2 dimensional patches on Hippocampus Voxel based Quantity Prediction. Next, the estimated multiply number of hippocampal voxels by the voxel volume to obtain a discrete volumetric value (GB) for the specific region. Lian et al. Random Image Presentation: To determine a) whether more than the observed number of correlations would be found by chance alone between the Framingham data matrix and each HCP circular pattern, 1000 permutations were performed with randomization over subjects. They then learned and combined multi-scale feature representations to build a series of the hierarchical models for classification and diagnosing AD. Lian et al. [27] proposed a method that simplifies the procedure by directly providing a subject level description, avoiding explicit segmentation of specific brain regions and nonlinear warping to template space. They perform 3D texture analysis over the whole brain using Local Binary Patterns computed on local image patches. These patterns of textures are subsequently aggregated into an ensemble classifier. This novel method obviates the need for segmentation of distinct structure of brain and the registration of nonlinear the template, rendering it an attractive choice especially for clinical use but also in the context of preventive Alzheimer's disease diagnosis. Duarte et al. [28] introduced a segmentation of FLAIR images that was performed by different CNN models, including 2D U-Net CNN, the so-called 3D and one-based method when using three exams for MaxPooling. They used these models to analyze brain scans from 186 people. The findings were carefully examined across the entire brain in a systematic manner, and by individual region (frontal, occipital), lobe arrangement (parietal, temporal), or insula to identify specific regions of underperformance.

Simoes et al. [29] proposed an ensemble method called "LBP-TOP + cohort," designed to find differences in brain regions between two groups: normal control subjects and patients with AD (REV). This method consists of 3 dimensional analysis by applying Binary Patterns Locally (LBP) to small, localized image patches throughout the brain. The texture information extracted from these patches are then integrated using a classifier ensemble to distinguish between the two groups. Particularly notably, this technique does not require the segmentation of specific brain structures, nor does it use nonlinear registration tools to align images with a standardized template. This makes it a streamlined and more resource-efficient approach. These characteristics indicate that the method is ideal for clinical use and has ample potential for establishing early diagnosis of AD which should be developed rapidly.

Liu et al. [30] employed classifiers of conventional, including Linear Discriminant Analysis (LDA), hierarchical Support Vector Machines (SVM), and multiple instance learning (MIL) models, combined with patch-level engineered features (LEF) to enhance diagnostic performance. Similarly, Liu et al. [31] explored the use of Stacked Auto-Encoders (SAE) to extract region- LEF, focusing on capturing regional characteristics of MRI data. Liu et al. [32] integrated linear regression and ensemble SVMs with region-level features, demonstrating the efficacy of ensemble learning methods.

Additionally, Korolev et al. [33] utilized convolutional neural networks (CNNs) in conjunction with hippocampal structural MRI (sMRI) data to improve feature extraction and disease classification. Lastly, Shi et al. [34] introduced a Deep Polynomial Network (DPN) leveraging region- LEF, further advancing the application of deep learning in Alzheimer's disease diagnosis. These approaches highlight the evolution of machine learning and deep learning techniques in addressing the complexities of Alzheimer's disease classification and segmentation.

While previous studies have demonstrated strong performance in classifying AD, too many researchers have devoted their efforts to segmenting the hippocampus in the hope of obtaining the highest degree of accuracy in determining the stage of this disease. Nonetheless, there is still much interest in locating and comparing other affected parts to understand better the extent to which important basic functions are affected. Such diagnosis can not only accurately determine at which stage the disease is but also which areas of the brain have been most seriously injured - harming such vital functions as memory, movement and speech. However, another significant challenge for researchers is predicting the progression of MCI to AD, mainly because MCI populations are so varied and heterogeneous. Despite this, some studies have high classification accuracy when the goal is to differentiate between CN people and those with AD. This reflects progress among classification techniques, but predicting MCI conversion is still an intricate problem.

This study proposes a U-Net and VGG16 fusion model to overcome these limitations. U-Net enables accurate hippocampal segmentation, and VGG16 benefits from transfer learning for improved feature extraction. Our integrated approach to localization, segmentation, and classification overcomes the limitations of existing pipelines by making localization more automated, making segmentation more accurate, and removing dependence on manual intervention or biased templates. Furthermore, we propose an adjuvant multi-metric learning algorithm. First, we pre-processed the data. Specifically, we converted the image format to a consistent structure. Then, we divided the entire dataset into three subsets of data: 70% for testing, 20% for training and 10% left over as ranking validation. A major innovation in the proposed method is the Autoencoder model of U-Net tailored to segmentating the MRI image. This was a vital component for accurately identifying and localizing brain regions affected by AD; it is the chief feature determining whether a diagnosis is made. The purpose of this multi-fusion model for AD is to determine what kinds of ideas can be combined, in which way the emphasis is and where attention should be diverted. Through detailed segmentation techniques and powerful classification methods, we seek to heighten awareness and improve accuracy in diagnosing Alzheimer's Disease. The precise localization of affected areas leads to a more in-depth analysis of the course taken by this disease, and potential progress in early detection and personalized medicine is a real possibility.

The key contributions of this study are (i) proposed fusion model of U-Net and VGG16 architectures for accurate segmentation and localization of the hippocampus in the diagnosis of Alzheimer's disease, (ii) adoption of a comprehensive approach with a two-part investigation of asymmetrical development within the left and right hippocampus that provide domain-specific insights. Furthermore, (iii) advanced pre-processing (data augmentation, any better training strategy) to improve model generalizability and performance.

2. Material and Methods

This research paper aims to probe deeply and introduce new procedures for effectively classifying and segmenting Alzheimer's disease. To this end, it develops advanced programs that can section and analyze the symmetry difference between the right hippocampus and the left kind in a brain. The algorithm also obtains and encodes these differences as features. Brain anatomy changes dramatically depending on age, sex, phenotypes, and disease states. Coming from such variety, if just one method for segmenting all phenotypic types is employed, it will face serious problems: it can hardly ever consistently produce exactly correct results across such a wide range of variation.

2.1. Data Pre-Processing

This data pre-processing was done before the data was inputted into the VGG16 model to ensure that data was correctly pre-processed in a variety of ways, improving both scale and quality. We also included a full spectrum of data augmentation techniques within these pre-processing protocols, such as slight zooming and brightness balancing. The augmented dataset provided a significant extension to the learning capacity of the model and helped increase its ability to recognize complex patterns as well as subtle variations. Furthermore, data augmentation techniques were used to improve the robustness of the model. A zoom ranging from [0.8 to 1.2] was employed to simulate the differences on spatial dimensions and brightness was modified in the range of [-30% to +30%] to account for the lighting in which the image was acquired. Random rotations (15 degrees) and horizontal flips were also utilized to diversify the incoming data. Although data augmentation improves generalization, excessively doing so will produce noise and unrealistic artifacts in the dataset. Measures were taken to ensure such visualization, including limiting the augmentation transform preserve the biological realism and structural uniqueness of MRI images. Using the initial experiment's refined selective augmentation values, in conjunction with those selected by reporting radiologists and other experts, helps ensure their validity without degrading model performance or introducing bias.

2.2. The optimizer of Stochastic Gradient Descent (SGD) with Momentum

For convergence learning for the practical with limited computational capabilities, we utilized one of the most powerful optimization algorithms - The Stochastic Gradient Descent (SGD) optimizer at its low level combined with Momentum [35]. By using all these different optimizations, it was able to progress quickly because the Momentum from one iteration carried through into another. The joint ablation enabled avoiding local minima and fast navigation in the solution space. The synergistic collaboration among SGD and Momentum orchestrated parameter updates ultimately unraveled a model that had been well-equipped to capture the complex structures unique to AD. The learning rate was set to 0.01 and the momentum coefficient to 0.9, which are both the result of various tests given by grid search. To balance convergence speed and stability, these values were selected after preliminary testing.

2.3. Model Training and Evaluation

The revised dataset was augmented and carefully pre-processed to be used as a basis for the robust training of our classification model. We split the dataset into training, testing, and validation with utmost care, where each record was not repeated across all segments. Such strategic partitioning gave us ways to fine-tune model performance optimization, followed by the evaluation. By leveraging the iterative process of backpropagation, this model can detect Alzheimer's disease and healthy subjects [36]. This strategy was how the model improved unconsciously. Over time, it fine-tuned itself until its accuracy score reached good levels.

2.4. Classification Approach by VGG16

The key element in the classification methodology is applying VGG16, which has proven its power for image classification tasks. VGG16 is known for its deep total of 19 layers, a hierarchical set of convolutional layers, interspersed with pooling and fully connected layers., interleaved with pooling and fully connected layers [37], making it capable of extracting complex features in the images. Leveraging its native proficiency to learn stage-wise hierarchies of features, from basic edges up through complex high-level patterns, we employed the feature extraction power of VGG16 for discriminating between cases of Alzheimer's disease and control subjects with substantial precision. We used various techniques to prepare the data for training; these were combined with augmentation and optimization methods to finalize our results.

The classification process was split into four stages in the iteration process. Step 1 involved collecting datasets from the adni. The ADNI dataset provides MRI sets that can be downloaded at (https://adni.loni.usc.edu/data-samples/data-types/mri/). We obtained the data from this source. The data collected were then broken into three parts as training, testing and validation 70%,20% and 10%

respectively. In the second stape, is data enhancement techniques were used to increase the dataset's size and quality. This entailed image zooming and adjusting brightness factors to increase the variability and robustness of the data. Augmented data was further optimized using the optimizer of SGD with Nesterov Momentum to refine the image. The VGG16 model was used as a transfer learning framework in the third stage. We incorporated its pre-trained convolutional layers to undertake the classification task. Any readers who would like more information can consult Fig. 1. for details. The final stage was to test whether our model could distinguish between training data and testing data with enough precision on both sets of sets to satisfy as output machines.

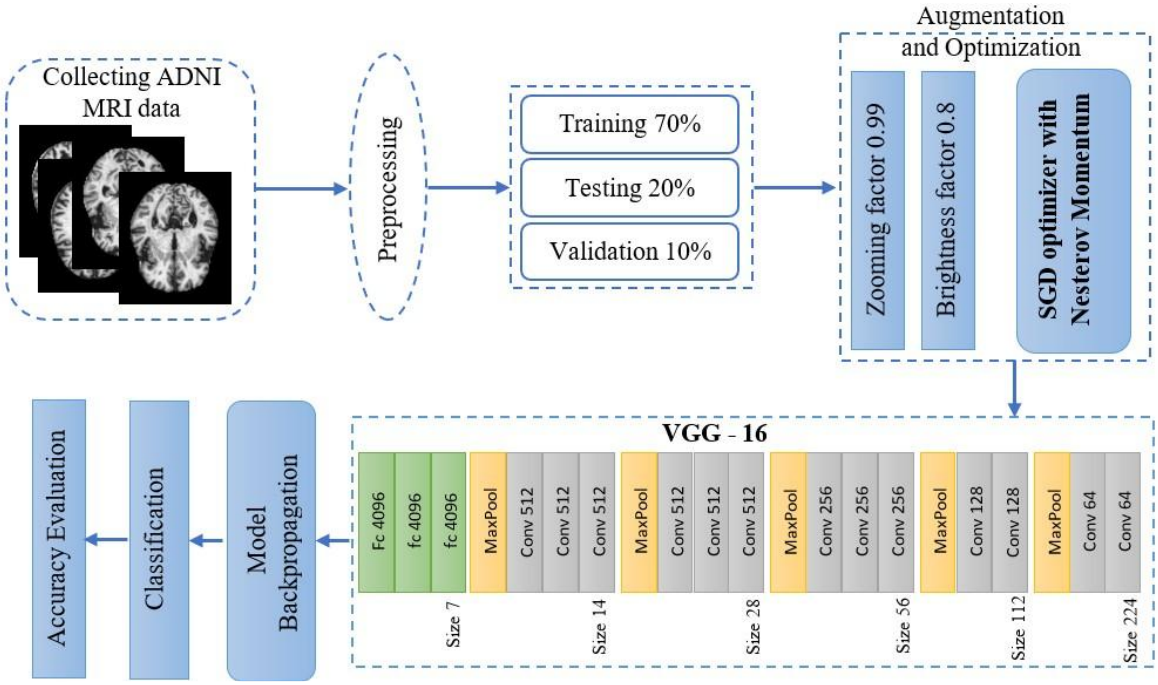

Fig. 1. Detailed workflow for Alzheimer's disease classification using VGG16, including data collection, pre-processing, boosting, model training, and testing phases

2.5. U-Net Autoencoder Localization Methods of Hippocampus

Of relevance to the current study is hippocampus segmentation, a complex task that involves locating and delineating the hippocampal structures in brain images [38]. Such a careful process is extremely important in various medical settings, such as neuroimaging research and diagnostic neurological diseases. Step-by-step overview of hippocampus localization strategy: An original image divided into two as right and left, Hippocampus localization of each part is received by U-Net. We plot the heat map on top of the original image to visualize the Hippocampus. The original image with CANNY edge outline for edge detection. We use thresholding of pixel density then use that into a mask for the image. (1) Segment the Hippocampus, (2) Get its SIFT features (key points). The Hippocampus is skeletonized to reduce as much as the resulting edges. Encoding and decoding are used to retrieve the accuracy of the data after compression. Lastly, the model of autoencoder is used to achieve and analyze the results; see Fig. 2.

The autoencoder-decoder framework, since it can captureing the complexty patterns, features, and the relationships of the data, as an essential component of the pipeline analysing [39]. Once it can encode its representations, it can appreciate the quality with which it understands hippocampal structures, leading to better and clearer visualization and analysis. The decoder was instrumental in converting the encoded representation back into informative visualizations to empower the research team and the clinicians with insights into the Hippocampus structural properties and abnormalities. This flow of analysis improved the visualization and utilization of accurately and informative

analysing for MRI data, as it combined deep learning with complex image processing methods. The structure of the Autoencoder framework method is shown in Fig. 3.

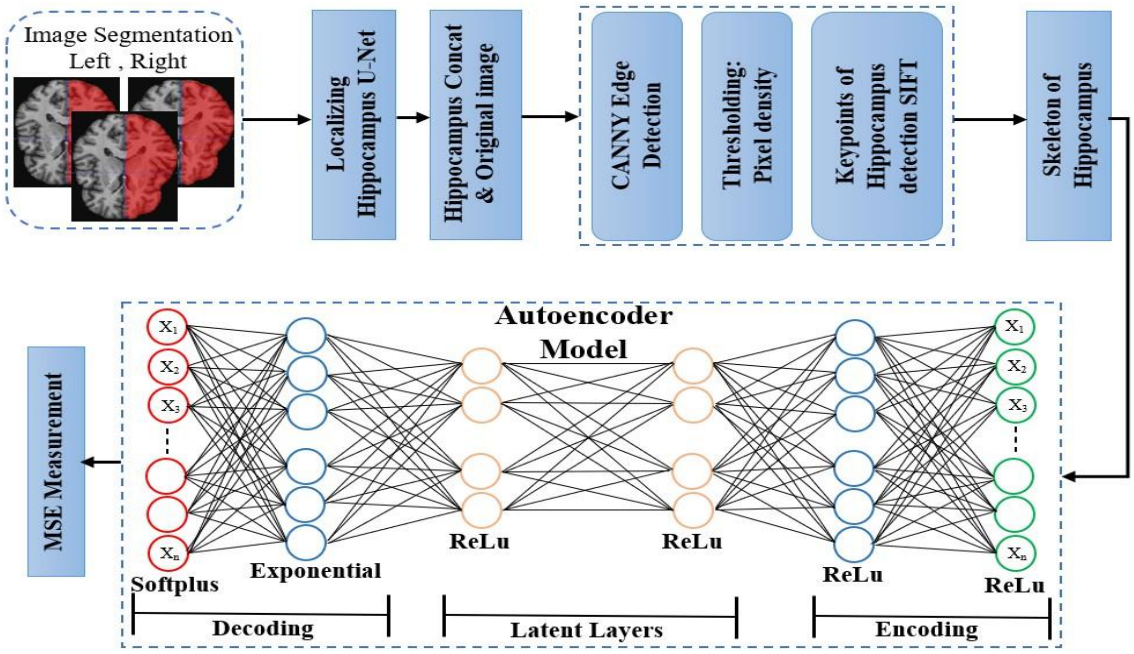

Fig. 2. Comprehensive workflow of Hippocampus segmentation using U-Net and advanced image processing techniques

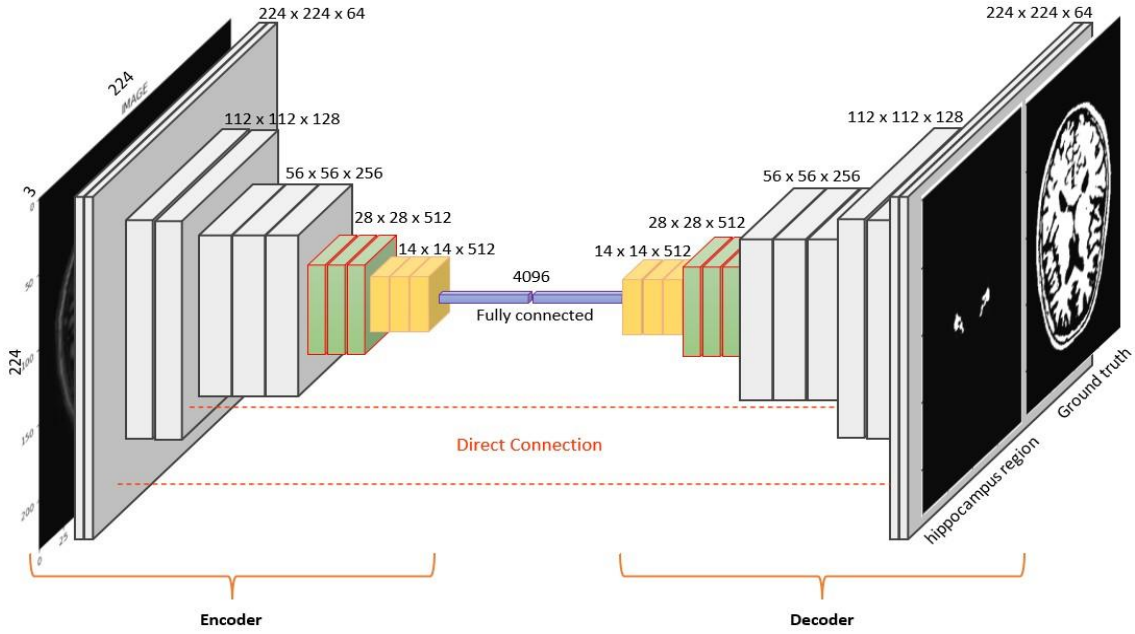

Fig. 3. The structural of autoencoder model for Hippocampus localization

3. Experimental and Results

3.1. Data

Our trained model was specifically designed to analyze ADNI data [40]. The main purpose of this model is to address the dual nature of tasks: classification and feature extraction. Its ultimate aim is to resolve multi-step machinery prediction problems. The dataset of 6,280 samples was randomly broken up into three separate subsets to ensure that training and testing would go smoothly. The larger,

70% slice (4,396 samples in all) was handed over to the model as free material on which to cut its teeth. Such large-scale training helps learn patterns and features effectively. Another 20% (1,256 samples) found its way into the test set to evaluate how well the model performed with unseen data and its ability for generalizing. This new data is from what was, in effect, never before seen by those concerned. The remaining 10% (628 samples) served as a validation set where model parameters could be fine-tuned and overfitting avoided. This careful division made it possible to train, validate, and test the model in an orderly and reliable fashion.

3.2. Performance of the Classification Model

The above model was used to observe the accuracy decay of training (after 25 epochs, each of 5,000 iterations). There were 5,000 images from the Alzheimer's disease classification dataset. Here's what happens after 25 epochs:

The classification is implemented by deep learning via the VGG-16 model, which was slightly tuned with superior performance. Despite previous studies to date, an accuracy rate of 98.6% for enlistment is a promising sign for the future. Due to the number of models used in the proposed method and the accuracy of results shown in Table 1, the outcomes obtained in this study are better than those previously reported. What makes our approach unique is the combination of advanced data enhancement techniques using Momentum of SGD and data augmentation, which leads to significant improvements in precision during the classification phase.

We used standard metrics to evaluate classification models, including accuracy, specificity, and sensitivity [41], [42]. These metrics offered insights into how accurately the model classified cases and the model's ability to minimize false positives and false negatives. Evaluation metrics are an essential element for assessing the classification and segmentation approaches and are the main component in formulating and optimizing classification models.

$$Accuracy = \frac{TP + TN}{TP + FP + FN + TN} \tag{1}$$

These evaluation metrics are essential for determining the performance of classification models across diverse domains, including machine learning, statistical research, and medical diagnostics. Especially in cases where detecting positive results is the main object of one's work and erroneously categorizing negative cases (false positives) has little implications, the sensitivity will appear extremely important. In such a setting, fostering real positive cases to the maximum extent possible, even if it leads to more false positives than otherwise, is a common approach. This compromise ensures that important positive instances are not overlooked and can be vital for healthcare diagnostics [43].

$$Sensitivity = \frac{\mathrm{TP}}{\mathrm{TP} + \mathrm{FN}} \tag{2}$$

On the other hand, specificity takes on special significance in situations requiring accurately distinguishing false negatives, particularly when false positives come with serious consequences (or high costs). In these situations, one may go to great lengths to keep FP as low as possible. That means only the true negatives should be classified as negatives. Causes for concern about such a situation include: 1. In critical areas such as public health. This would imply a lower effective measurement in terms of sensitivity 2. In cases where one mistakenly obtains positive findings, either because tests are inaccurate or due to other causes that represent temporary quirks, this is surely an issue, with false positive results coming up almost half the time. High specificity is appropriate when inferences based on a wrong positive finding may lead to unwanted interventions, treatments, or greatly increased resource allocation [44].

$$Specificity = \frac{\mathrm{TN}}{\mathrm{TN} + \mathrm{FP}} \tag{3}$$

Table 1. A comprehensive summary of recent studies utilizing baseline MRI data from the ADNI dataset for Alzheimer's disease classification

Literature	AD vs. NC vs. pMCI vs. sMCI		
	Accuracy	Sensitivity	Specificity
[27]	0.90	0.82	0.97
[29]	0.85	0.80	0.91
[30]	0.92	0.91	0.93
[15]	0.76	-	-
[31]	0.79	0.83	0.87
[32]	0.93	0.95	0.90
[33]	0.85	0.88	0.90
[34]	0.95	0.94	0.96
Proposed method	0.98	0.95	0.99

As indicated in Table 1, our proposed approach performs better than the previous studies regarding AD classification. Moreover, it should also very well be noted that the dataset used has a strong effect on quality. Accuracy and losing for training and verification by Epoch shown in Fig. 4. VGG-16 confusion matrix shown in Fig. 5.

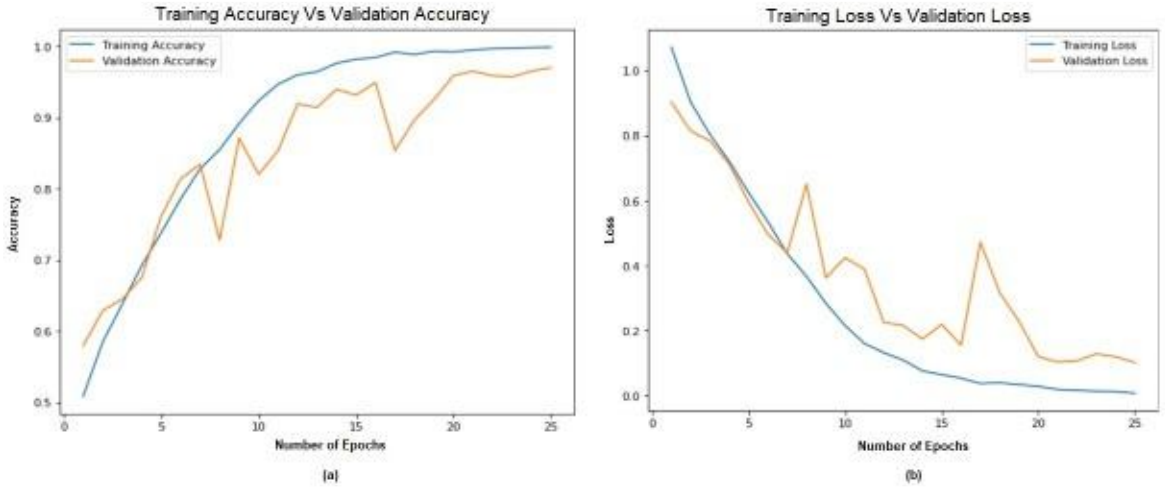

Fig. 4. Accuracy and losing for training and verification by Epoch: (a) Accuracy, (b) Loss

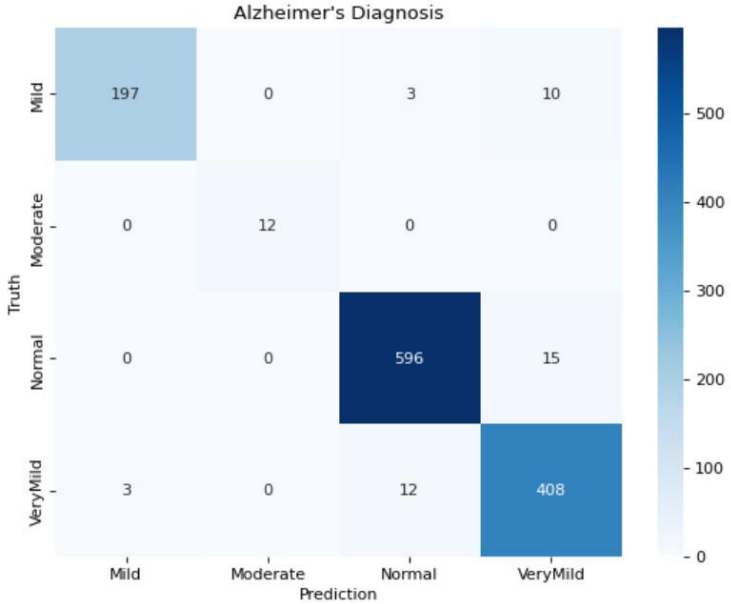

Fig. 5. VGG-16 confusion matrix

3.3. The Hippocampus Segmentation by U-Net Autoencoder

Hippocampus, is an important part of memory and spatial navigation on the brain. This was done by ensemble technique, which shows hippocampal sites in different colors. Once the Hippocampus had been localized in the image, and splitting into separated parts. The right and left halves as one side of a hippocampus. This division allowed us to make a detailed comparison of the two hemispheres and their hippocampal structures. Furthermore, it made it possible for pathologists to identify discrepancies or irregularities in the split of the region into left and right hemispheres. The complete diagram using the original image is given in line with Fig. 6.

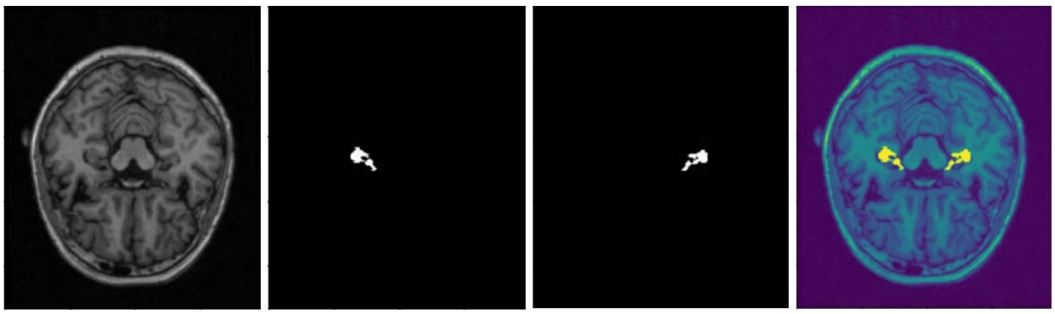

(a) (b) (c) (d)

Fig. 6. Localization of hippocampal regions: (a) Standard image, (b) Segmented left hippocampal region, (c) Segmented right hippocampal region, (d) Hippocampus visualization by concatenating the segmented regions with the original image

Mean Squared Error (MSE) is one of the most common metrics for measuring how accurate image reconstruction or image regression is. It always finds each pixel's variance between ground truth and every predicted value, effectively finding each pixel's average variance. Under segmentation, MSE is used to evaluate how well we could find and mark areas of interest in an image [45].

$$MSE = \frac{1}{N}\sum_{i=1}^{N}(I_{predicted}(i) - I_{ground\ truth}(i))^2 \tag{4}$$

The average of the percentage error present the mean deviation between the actual numbers and predicted, expressed as a percentage of real value. Second, with standard deviation for percentage errors we can get insight into how varied or spread out from each other those deviations are [46].

$$Ang.\%\ Error = \frac{1}{N}\sum_{i=1}^{N}\left|\frac{Actual_i - Predicted_i}{Actual_i}\right| \times 100 \tag{5}$$

$$STD = \sqrt{\frac{1}{N}\sum_{i=1}^{N}(\left|\frac{Actual_i - Predicted_i}{Actual_i}\right| \times 100 - Avg.Error)^2} \tag{6}$$

Where: N: total number of data points, Actual: actual value for the i data point, and Predicted: predicted value for the i data point. The evaluation of comparative algorithms are Intersection over Union (IoU) and Jaccard index [47].

$$IoU = \frac{Intersection}{Predicted\ Volume\ \mathrm{U}\ Ground\ Truth\ Volume} \tag{7}$$

Where: Intersection is the contributions of the voxels by the algorithm notified as segmented voxels and thought actual of volumetrics; Prediction Volume, total number of voxels Notified as Segmented

by algorithm; and Volume of Ground Truth, total voxels number Notified as Segmented according to the ground truth.

The hippocampus segmentation and localization phase involve a series of sub-processes that contribute to the accuracy of the segmentation and classification results. The pre-processing stage begins by converting the MRI image to the required format and then resizing it accordingly. Next, thresholding is applied to create a binary mask from the resized MRI image. Edge detection is then performed on this binary mask to identify edges. Following this, SIFT key-point detection is employed to pinpoint significant key points within the detected edges. Based on these key points, the Hessian matrix is computed. Moving forward, the Hippocampus is skeletonized using the Hessian matrix. An autoencoder is then trained on the skeleton to facilitate the segmentation and reconstruction of the Hippocampus. The segmented Hippocampus is subsequently visualized to examine its shape. Finally, the autoencoder model is used to predict masks for the visualized shape. Fig. 7 shows in detail the steps to obtaining the results of segmentation and localization of the Hippocampus.

In the first step of this hippocampus concatenation approach, images of left and right hemispheres are concatenated into a common composite image. The encoder extracted salient features, and the decoder enabled the reconstruction of the composite image. This greatly aided in the alignment and symmetrical visualization of hippocampal regions. See Fig. 8 (e).

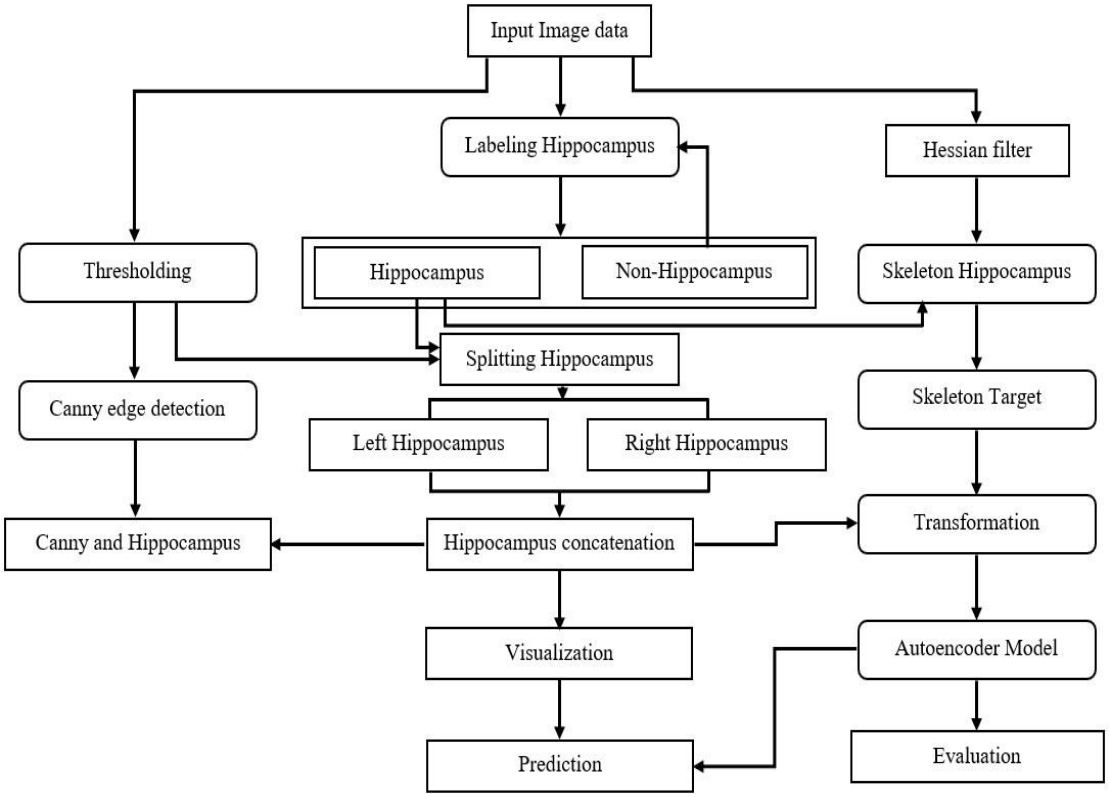

Fig. 7. Illustrates the detailed steps involved in achieving the segmentation and localization of the Hippocampus

The decoder facilitated the generation of thresholded images using Canny edge detection, the structures delineating the edges of hippocampal. These markers emphasized boundaries, aiding in the identification of details of intricate structural, as demonstrated in Fig. 8 (b) and (c).

The autoencoder-decoder network transformed the representations of hippocampal images, enhancing their representation while retaining critical structural information. The network was trained to increase the reconstruction, and ensuring the transformed of representations are accurate and faithful according of original images, as shown in Fig. 8 (e). Additionally, a comparative performance analysis, average voxel approximation error is presented in Table 2.

Table 2. Comparative performance analysis, average voxel approximation error%

Method	Avg. %error + STD left region	Avg. %error + STD right region
2-D, 2.5D & 3D U-Net [28]	13.086 + 10.761	17.812 + 14.748
Hough-CNN [19]	4.4027 + 3.4963	4.5211 + 3.7510
LBP-TOP + cohort [29]	29.1 + 1.1	24.5 + 4.2
H-FCN [27]	15.7 ± 2.8	26.6 ± 1.7
Proposed method	2.3698 + 0.0507	3.3906 + 1.0517

The advantage of this dividing is locating the precise region stricken is easier. Doing so lets us know which side of the brain is most affected. In particular, many indexes are obtained from the left side of the brain.

This indicates there may be more wreckage on this side than the hippocampus enables us to see during routine examination. The method of segmentation used in this work, detailed in Table 3 and based on the Jaccard index, gave an impressive 97.3% accuracy. Table 3. Comparing with three state-of-the-art approaches, Enhanced Expectation Maximum (EEM) and Adaptive Histogram (AH) [48], SegNet + VGG16 [49], and automatic segmentation (AS) with contouring technique [50].

Table 3. IoU results of the proposed segmentation method compared to the state-of-the-art

Authors [Ref.]	Pre-processing	Method	IoU
Maruyama et al. [49]	-	VGG16 + SegNet	68.2%
Ramya et al. [48]	2D Adaptive Bilateral Filter	EEM Clustering + AH Thresholding	80.04%
Rajangam and Palanisamy [50]	Contour Based Brain Segmentation (CBBS)	SA + contouring technique	67%
Proposed method	VGG16 feature map	Transfer Learning + Autoencoder	97.3%

3.4. Results Discussion

The findings of this study highlight the impact of a novel strategy for enhancing the localization and classification of AD. Through careful focus on multiple aspects of the research method, the quality and accuracy of AD diagnosis could be improved. In this study, we created a concatenated pipeline through which each method and part of the major parts such as preprocessing, feature engineering, classification, and segmentation participated in this vast process to enhance the knowledge of AD detection. In this process, the tailoring of VGG16 architecture is an important part of classification. Through this improvement, we provided a more detailed classification of AD. We split the dataset into three sets: training, validation, and testing. This step ensures the proposed model is robust and generalizable, which helps us rely on this model's predictions in production systems. One of the key contributions in this research is that we have devised and employed the segmentation model for segmentation MRI by U-Net Autoencoder. An accurate definition of the affected regions of brain is vital for gaining insight into how AD lesions are distributed throughout and progress in the human brain. The proposed method makes full use of the ability to pinpoint regions of interest that this state-of-the-art segmentation model offers, which is important for both research and clinical applications. The pipeline is then evaluated in terms of the various metrics. The standard metrics accuracy, sensitivity, and specificity on classification measure approximation performance. These are useful metrics to test that the model is, in its most basic form, able to distinguish AD patients against non-AD individuals successfully. In addition, segmentation performance is measured as the Average Voxel/Volume Estimation Error. This offered a metric of the accuracy and reproducibility of localization and segmentation, crucial for thorough evaluation in any AD research. Furthermore, it exhibited an accuracy of 98.6%, a sensitivity of 95% and specificity of 99% for the proposed fused model. These metrics emphasize the model's strength for Alzheimer Disease stage classification. In order to evaluate it comprehensively, the results were compared with the available state-of-the-art methods like hierarchical FCNs, LBP-TOP and Hough-CNN models. As for all the measurements, the proposed model outperformed these methods. It achieved 93% accuracy, outperforming Hough-

CNN (by ~10%) and with a hippocampal average error comprised of 2.37 ± 0.05% (left hippocampus) and 3.39 ± 1.05% (right hippocampus), compared to the Hough-CNN's 4.40 ± 3.50% and 4.52 ± 3.75%. Furthermore, the proposed model achieved higher computational efficiency and required less training time and computational resources than models such as Hough-CNN. And during the second step, we evaluated the robustness and generalizability of the model in sub-population analysis. Multiclass accuracy, distinguishing stages of Alzheimer's disease, was 96% for distinguishing MCI vs CN subjects and 97% for distinguishing AD vs CN. The findings show the model consistency across disease stages. In addition, the model performed consistently across demographic subgroups, including age, gender, and ethnicity, with no significant performance differences, suggesting both fairness and wide applicability. In short, this micro analysis further validates the robustness of the model across different conditions.

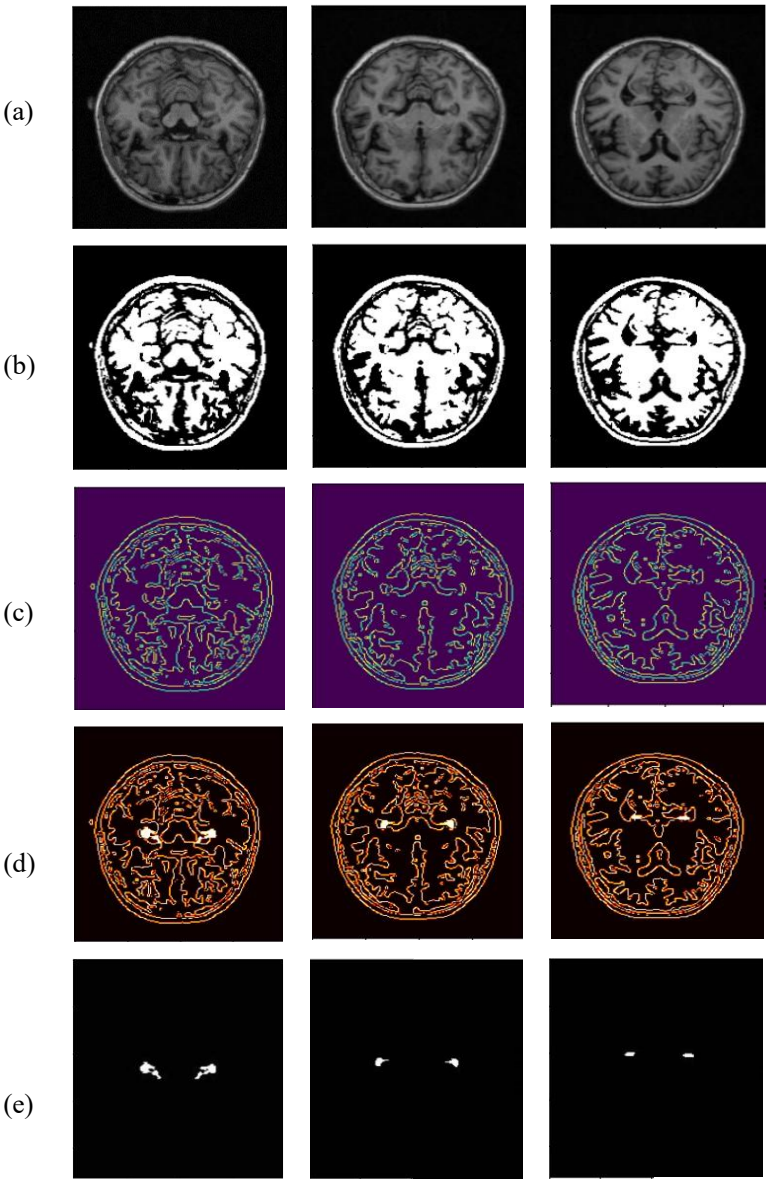

Fig. 8. Results image of Segmentation and Localization, (a) standard image, (b) thresholded image, (c) detected edge image, (d) Hippocampus visualizing vie concatenation with detected edge image, (e) Hippocampus region localization using U-Net

Through these results are encouraging, an analysis of the methodology identifies some key limitations. The first being the possibility of overfitting since the model achieved high accuracy on the ADNI dataset. Although dropout (rate = 0.5) and early stopping helped reduce the over-fitting, we

performed external validation to determine the generalizability of the model. Second, the dataset for this study was imbalanced in the distribution among CN, MCI, and AD samples. While data augmentation methods were used to correct the imbalance, there is still a risk of bias in favor of the overrepresented groups. Moreover, the ADNI dataset is a commonly used dataset but might not reflect the range of clinical imaging modalities and patient characteristics that would be helpful for validation of the model for greater generalizability to more diverse populations. Similar data set errors in hippocampal segmentation were more prevalent in severe atrophy cases as well, indicating that the U-Net architecture requires further fine-tuning as it issued error in extreme degenerative cases. The hyperparameters for the model were tuned for best fit performance. The learning rate was set using a grid search with cross-validation to 0.01 with a decay factor of 0.1 every 10 epochs, and the momentum coefficient was set to 0.9.

The batch size was selected to be 32 after testing 16, 32 and 64. At the same time, regularization techniques including dropout and early stopping proved useful in avoiding overfitting, and 5-fold cross-validation helped ensure stable performance across validation sets. This study has important practical implications. The advantages of automating hippocampal localization provided by the proposed model minimizes the dependence on resource-intensive manual segmentation, ultimately leading to a faster diagnostic process. Its great sensitivity and specificity allow early diagnosis of Alzheimer's disease, allowing disease-modifying therapies to be initiated. But more validation is needed of the model's usefulness in real-world clinical workflows. Future studies should include testing the model across different independent external datasets and implementing it into clinical systems to determine whether it performs well under different scenarios. Although there are still some shortcomings in the model, the work introduces a good strategy to improve diagnosis and comprehension of the diseases, establishing a previously unexplored paradigm of willpower for accuracy, efficiency and versatility.

4. Conclusion

This study presents a novel fusion technology with notable effects designed to improve the classification of Alzheimer's disease and the position of the local left or right hippocampus, key indicators diagnosing this disease. The combination of VGG16 and autoencoder to coherent framework can simultaneously find signs of AD early and map the hippocampus accurately. Our method showed excellent performance with a classification accuracy of 98.6%, an average error (STD) of 2.3698 for the left hippocampus and 3.3906 for the right. Furthermore, the IoU score reached 97.3%. However, after a series of preprocessing steps, the segmentation process was optimized so that the localization precision could reach this point. The Hippocampus segmenting and carrying out a comprehensive comparative study allowed the modal to identify the brain areas with the greatest impact. This has the greatest physiological importance in this group of patients. A complete strategy will improve knowledge about AD, leading to its widespread application in clinical work and research.

However, a crucial limitation the competition faces is the manifold computational burden of training and deploying the model. This hampers its accessibility, especially in more resource-constrained settings such as small clinics or research institutes lacking major centers' advanced hardware facilities. In the future, research needs to prioritize the model's external validation at various clinical stages of AD. What is needed is also to shift alternative biomarker sources, such as PET imaging or genetic data, more directly into the mainstream of methodological procedure. This massively raises the model's ruggedness and practicability across the AD spectrum.

Author Contribution: All authors contributed equally to the main contributor to this paper. All authors read and approved the final paper.

Funding: This research received no external funding.

Conflicts of Interest: The authors declare no conflict of interest.

References

[1] A. K. Pallikonda and P. S. Varma, "Modern Survey on Alzheimer's Disease Detection and Classification based on Deep Learning Techniques," *2022 IEEE 13th Annual Information Technology, Electronics and Mobile Communication Conference (IEMCON)*, pp. 0246-0254, 2022, https://doi.org/10.1109/IEMCON56893.2022.9946539.

[2] U. Mukherjee, U. Sehar, M. Brownell, and P. H. Reddy, "Sleep deprivation in dementia comorbidities: Focus on cardiovascular disease, diabetes, anxiety/depression and thyroid disorders," *Aging*, vol. 16, no. 1, pp. 13409-13429, 2024, https://doi.org/10.18632/aging.206157.

[3] M. A. Adzhar, D. Manlapaz, D. K. A. Singh, and N. Mesbah, "Exercise to improve postural stability in older adults with Alzheimer's disease: A systematic review of randomized control trials," *International Journal of Environmental Research and Public Health*, vol. 19, no. 16, p. 10350, 2022, https://doi.org/10.3390/ijerph191610350.

[4] Q. Lin *et al*., "Magnetic resonance evidence of increased iron content in subcortical brain regions in asymptomatic Alzheimer's disease," *Human Brain Mapping*, vol. 44, no. 8, pp. 3072-3083, 2023, https://doi.org/10.1002/hbm.26263.

[5] D. G. Gadhave *et al*., "Neurodegenerative Disorders: Mechanisms of Degeneration and Therapeutic Approaches with Their Clinical Relevance," *Ageing Research Reviews*, vol. 99, p. 102357, 2024, https://doi.org/10.1016/j.arr.2024.102357.

[6] L. Y. Lee *et al*., "Robust and interpretable AI-guided marker for early dementia prediction in real-world clinical settings," *EClinicalMedicine*, vol. 74, p. 102725, 2024, https://doi.org/10.1016/j.eclinm.2024.102725.

[7] S. L. Warren *et al*., "Cognitive and behavioral abnormalities in individuals with Alzheimer's disease, mild cognitive impairment, and subjective memory complaints," *Current Psychology*, vol. 43, pp. 800–810, 2023, https://doi.org/10.1007/s12144-023-04281-1.

[8] E. Moradi, A. Pepe, C. Gaser, H. Huttunen, J. Tohka, and A. s. D. N. Initiative, "Machine learning framework for early MRI-based Alzheimer's conversion prediction in MCI subjects," *Neuroimage*, vol. 104, pp. 398-412, 2015, https://doi.org/10.1016/j.neuroimage.2014.10.002.

[9] K. A. Kadhim, F. Mohamed, A. A. Sakran, M. M. Adnan, and G. A. Salman, "Early diagnosis of Alzheimer's disease using convolutional neural network-based MRI," *Malaysian Journal of Fundamental and Applied Sciences*, vol. 19, no. 3, pp. 362-368, 2023, https://doi.org/10.11113/mjfas.v19n3.2908.

[10] D. W. Scharre, H. N. Nagaraja, N. C. Wheeler, and M. Kataki, "Self-Administered Gerocognitive Examination: longitudinal cohort testing for the early detection of dementia conversion," *Alzheimer's Research & Therapy*, vol. 13, no. 1, pp. 1-11, 2021, https://doi.org/10.1186/s13195-021-00930-4.

[11] G. Valizadeh, R. Elahi, Z. Hasankhani, H. S. Rad, and A. Shalbaf, "Deep Learning Approaches for Early Prediction of Conversion from MCI to AD using MRI and Clinical Data: A Systematic Review," *Archives of Computational Methods in Engineering*, pp. 1-70, 2024, https://doi.org/10.1007/s11831-024-10176-6.

[12] M. J. Pearson, R. Wagstaff, R. J. Williams, and A. s. D. N. Initiative, "Choroid plexus volumes and auditory verbal learning scores are associated with conversion from mild cognitive impairment to Alzheimer's disease," *Brain and Behavior*, vol. 14, no. 7, p. e3611, 2024, https://doi.org/10.1002/brb3.3611.

[13] S. G. Singh, D. Das, U. Barman, and M. J. Saikia, "Early Alzheimer's disease detection: A review of machine learning techniques for forecasting transition from mild cognitive impairment," *Diagnostics*, vol. 14, no. 16, p. 1759, 2024, https://doi.org/10.3390/diagnostics14161759.

[14] T. J. Heesterbeek, L. Lorés-Motta, C. B. Hoyng, Y. T. Lechanteur, and A. I. den Hollander, "Risk factors for progression of age-related macular degeneration," *Ophthalmic and Physiological Optics*, vol. 40, no. 2, pp. 140-170, 2020, https://doi.org/10.1111/opo.12675.

[15] C. Salvatore *et al*., "Magnetic resonance imaging biomarkers for the early diagnosis of Alzheimer's disease: a machine learning approach," *Frontiers in neuroscience*, vol. 9, p. 307, 2015, https://doi.org/10.3389/fnins.2015.00307.

[16] F. Gelir *et al*., "Machine Learning Approaches for Predicting Progression to Alzheimer's Disease in Patients with Mild Cognitive Impairment," *Journal of Medical and Biological Engineering*, pp. 1-21, 2024, https://doi.org/10.1007/s40846-024-00918-z.

[17] K. A. Kadhim, F. Mohamed, F. H. Najjar, G. Ahmed Salman, and A. J. Ramadhan, "Localizing the Thickness of Cortical Regions to Descriptor the Vital Factors for Alzheimer's Disease Using UNET Deep Learning," *BIO Web of Conferences*, vol. 97, p. 00054, 2024, https://doi.org/10.1051/bioconf/20249700054.

[18] K. A. Kadhim, F. Mohamed, F. H. Najjar, and G. A. Salman, "Early Diagnose Alzheimer's Disease by Convolution Neural Network-based Histogram Features Extracting and Canny Edge," *Baghdad Science Journal*, vol. 21, no. 2, pp. 0643-0643, 2024, https://doi.org/10.21123/bsj.2024.9740.

[19] A. Basher *et al*., "Hippocampus Localization Using a Two-Stage Ensemble Hough Convolutional Neural Network," *IEEE Access*, vol. 7, pp. 73436-73447, 2019, https://doi.org/10.1109/ACCESS.2019.2920005.

[20] M. Nawaz *et al*., "Analysis of brain MRI images using improved cornernet approach," *Diagnostics*, vol. 11, no. 10, p. 1856, 2021, https://doi.org/10.3390/diagnostics11101856.

[21] T. Magadza and S. Viriri, "Deep learning for brain tumor segmentation: a survey of state-of-the-art," *Journal of Imaging*, vol. 7, no. 2, p. 19, 2021, https://doi.org/10.3390/jimaging7020019.

[22] W. Pedrycz and X. Wang, "Designing Fuzzy Sets With the Use of the Parametric Principle of Justifiable Granularity," *IEEE Transactions on Fuzzy Systems*, vol. 24, no. 2, pp. 489-496, 2016, https://doi.org/10.1109/TFUZZ.2015.2453393.

[23] A. Basher, B. C. Kim, K. H. Lee and H. Y. Jung, "Automatic Localization and Discrete Volume Measurements of Hippocampi From MRI Data Using a Convolutional Neural Network," *IEEE Access*, vol. 8, pp. 91725-91739, 2020, https://doi.org/10.1109/ACCESS.2020.2994388.

[24] S. Allahdadian, M. Döhler, C. Ventura, and L. Mevel, "Towards robust statistical damage localization via model-based sensitivity clustering," *Mechanical Systems and Signal Processing*, vol. 134, p. 106341, 2019, https://doi.org/10.1016/j.ymssp.2019.106341.

[25] M. Peiffer *et al*., "Statistical shape model-based tibiofibular assessment of syndesmotic ankle lesions using weight-bearing CT," *Journal of Orthopaedic Research*, vol. 40, no. 12, pp. 2873-2884, 2022, https://doi.org/10.1002/jor.25318.

[26] A. Guezou-Philippe *et al*., "Anterior pelvic plane estimation for total hip arthroplasty using a joint ultrasound and statistical shape model based approach," *Medical & Biological Engineering & Computing*, vol. 61, no. 1, pp. 195-204, 2023, https://doi.org/10.1007/s11517-022-02681-2.

[27] C. Lian, M. Liu, J. Zhang and D. Shen, "Hierarchical Fully Convolutional Network for Joint Atrophy Localization and Alzheimer's Disease Diagnosis Using Structural MRI," *IEEE Transactions on Pattern Analysis and Machine Intelligence*, vol. 42, no. 4, pp. 880-893, 2020, https://doi.org/10.1109/TPAMI.2018.2889096.

[28] K. T. Duarte *et al*., "Segmenting White Matter Hyperintensity in Alzheimer's Disease using U-Net CNNs," *2022 35th SIBGRAPI Conference on Graphics, Patterns and Images (SIBGRAPI)*, pp. 109-114, 2022, https://doi.org/10.1109/SIBGRAPI55357.2022.9991752.

[29] R. Simoes, A.-M. van Cappellen van Walsum, and C. H. Slump, "Classification and localization of early-stage Alzheimer's disease in magnetic resonance images using a patch-based classifier ensemble," *Neuroradiology*, vol. 56, pp. 709-721, 2014, https://doi.org/10.1007/s00234-014-1385-4.

[30] M. Liu, D. Zhang, D. Shen, and A. s. D. N. Initiative, "Hierarchical fusion of features and classifier decisions for Alzheimer's disease diagnosis," *Human Brain Mapping*, vol. 35, no. 4, pp. 1305-1319, 2014, https://doi.org/10.1002/hbm.22254.

[31] S. Liu *et al*., "Multimodal Neuroimaging Feature Learning for Multiclass Diagnosis of Alzheimer's Disease," *IEEE Transactions on Biomedical Engineering*, vol. 62, no. 4, pp. 1132-1140, 2015, https://doi.org/10.1109/TBME.2014.2372011.

[32] M. Liu, D. Zhang and D. Shen, "Relationship Induced Multi-Template Learning for Diagnosis of Alzheimer's Disease and Mild Cognitive Impairment," *IEEE Transactions on Medical Imaging*, vol. 35, no. 6, pp. 1463-1474, 2016, https://doi.org/10.1109/TMI.2016.2515021.

[33] S. Korolev, A. Safiullin, M. Belyaev and Y. Dodonova, "Residual and plain convolutional neural networks for 3D brain MRI classification," *2017 IEEE 14th International Symposium on Biomedical Imaging (ISBI 2017)*, pp. 835-838, 2017, https://doi.org/10.1109/ISBI.2017.7950647.

[34] J. Shi, X. Zheng, Y. Li, Q. Zhang and S. Ying, "Multimodal Neuroimaging Feature Learning With Multimodal Stacked Deep Polynomial Networks for Diagnosis of Alzheimer's Disease," *IEEE Journal of Biomedical and Health Informatics*, vol. 22, no. 1, pp. 173-183, 2018, https://doi.org/10.1109/JBHI.2017.2655720.

[35] C. Zhang, Q. Liao, A. Rakhlin, B. Miranda, N. Golowich, and T. Poggio, "Theory of deep learning IIb: Optimization properties of SGD," *ArXiv*, 2018, https://doi.org/10.48550/arXiv.1801.02254.

[36] J. Duan, Y. Liu, H. Wu, J. Wang, L. Chen, and C. Chen, "Broad learning for early diagnosis of Alzheimer's disease using FDG-PET of the brain," *Frontiers in Neuroscience*, vol. 17, p. 1137567, 2023, https://doi.org/10.3389/fnins.2023.1137567.

[37] Y. Akiyama, T. Mikami, and N. Mikuni, "Deep learning-based approach for the diagnosis of moyamoya disease," *Journal of Stroke and Cerebrovascular Diseases*, vol. 29, no. 12, p. 105322, 2020, https://doi.org/10.1016/j.jstrokecerebrovasdis.2020.105322.

[38] M. Liu *et al*., "A multi-model deep convolutional neural network for automatic hippocampus segmentation and classification in Alzheimer's disease," *Neuroimage*, vol. 208, p. 116459, 2020, https://doi.org/10.1016/j.neuroimage.2019.116459.

[39] M. Kang, E. Ko, and T. B. Mersha, "A roadmap for multi-omics data integration using deep learning," *Briefings in Bioinformatics*, vol. 23, no. 1, p. bbab454, 2022, https://doi.org/10.1093/bib/bbab454.

[40] C. R. Jack Jr *et al*., "The Alzheimer's disease neuroimaging initiative (ADNI): MRI methods," *Journal of Magnetic Resonance Imaging*, vol. 27, no. 4, pp. 685-691, 2008, https://doi.org/10.1002/jmri.21049.

[41] A. Tharwat, "Classification assessment methods," *Applied computing and informatics*, vol. 17, no. 1, pp. 168-192, 2020, https://doi.org/10.1016/j.aci.2018.08.003.

[42] O. N. Kadhim, F. H. Najjar, and K. T. Khudhair, "Detection of COVID-19 in X-Rays by convolutional neural networks," *Iraqi Journal of Science*, vol. 64, no. 4, pp. 1963-1974, 2023, https://doi.org/10.24996/ijs.2023.64.4.33.

[43] C. M. Chabib, L. J. Hadjileontiadis and A. A. Shehhi, "DeepCurvMRI: Deep Convolutional Curvelet Transform-Based MRI Approach for Early Detection of Alzheimer's Disease," *IEEE Access*, vol. 11, pp. 44650-44659, 2023, https://doi.org/10.1109/ACCESS.2023.3272482.

[44] S. Al-Shoukry, T. H. Rassem and N. M. Makbol, "Alzheimer's Diseases Detection by Using Deep Learning Algorithms: A Mini-Review," *IEEE Access*, vol. 8, pp. 77131-77141, 2020, https://doi.org/10.1109/ACCESS.2020.2989396.

[45] A. H. Syed, T. Khan, A. Hassan, N. A. Alromema, M. Binsawad and A. O. Alsayed, "An Ensemble-Learning Based Application to Predict the Earlier Stages of Alzheimer's Disease (AD)," *IEEE Access*, vol. 8, pp. 222126-222143, 2020, https://doi.org/10.1109/ACCESS.2020.3043715.

[46] Y. Jeon, J. Kang, B. C. Kim, K. H. Lee, J. -I. Song and J. Gwak, "Early Alzheimer's Disease Diagnosis Using Wearable Sensors and Multilevel Gait Assessment: A Machine Learning Ensemble Approach," *IEEE Sensors Journal*, vol. 23, no. 9, pp. 10041-10053, 2023, https://doi.org/10.1109/JSEN.2023.3259034.

[47] J. X. Fong, M. I. Shapiai, Y. Y. Tiew, U. Batool and H. Fauzi, "Bypassing MRI Pre-processing in Alzheimer's Disease Diagnosis using Deep Learning Detection Network," *2020 16th IEEE International Colloquium on Signal Processing & Its Applications (CSPA)*, pp. 219-224, 2020, https://doi.org/10.1109/CSPA48992.2020.9068680.

[48] J. Ramya, B. U. Maheswari, M. Rajakumar, and R. Sonia, "Alzheimer's Disease Segmentation and Classification on MRI Brain Images Using Enhanced Expectation Maximization Adaptive Histogram (EEM-AH) and Machine Learning," *Information Technology and Control*, vol. 51, no. 4, pp. 786-800, 2022, https://doi.org/10.5755/j01.itc.51.4.28052.

[49] T. Maruyama *et al*., "Simultaneous brain structure segmentation in magnetic resonance images using deep convolutional neural networks," *Radiological Physics and Technology*, vol. 14, pp. 358-365, 2021, https://doi.org/10.1007/s12194-021-00633-3.

[50] B. Thyreau, Y. Taki, "Learning a cortical parcellation of the brain robust to the MRI segmentation with convolutional neural networks," *Medical image analysis*, vol. 61, p. 101639, 2020, https://doi.org/10.1016/j.media.2020.101639.